treatment. The dosage levels were determined based on the results of the dose-finding study in young rats. Recovery groups (0 or 100 mg/kg per day) (6/sex per dose) were maintained for 2 weeks without chemical treatment and fully examined at 11 weeks of age. Rats were examined for general condition, BW, food consumption, urinalysis, hematology and blood biochemistry, necropsy findings, organ weights and histopathological findings. The study using young rats was conducted at Kashima Laboratory, Mitsubishi Chemical Safety Institute Ltd. (Kashima, Japan) under GLP conditions (MHW 1988; OECD 1997).

Statistical analysis

Continuous data were analyzed with Bartlett's test for homogeneity of variance. If the data were homogeneous, Dunnett's test was conducted for group comparisons between control and individual TNP-treated groups. If not homogenous, the data were analyzed using Steel's test. Quantitative data for histopathology were analyzed with Mann–Whitney's *U*-test or Fisher's exact test. In the newborn rat study, the chi-square test was conducted for physical and sexual development and reflex ontogeny. The 0.05 or 0.01 level of probability was used as the criterion for significance.

RESULTS

Repeated dose study in newborn rats (dose-finding study)

Death occurred at 81.4 mg/kg per day in one male on day 3 of the dosing period, two females on days 6 and 7 of the dosing period, and at 407 mg/kg per day in all rats by day 4 of the dosing period. In these dead rats, hypoactivity, bradypnea and hypothermia were observed. Only hypoactivity was found in surviving rats at 81.4 mg/kg per day on days 3, 5, or 8 of the dosing period. Yellowish fur was observed in all TNP-treated rats.

A significantly lower BW (max. 16% decreased) in males, and suppression of weight gain (max. 35% decreased) in females were noted at 81.4 mg/kg per day. The organ weights are summarized in Table 1. At 81.4 mg/kg per day, a significantly higher relative weight of the liver (13% increased) and lower relative weight of the kidney (14% decreased) were observed in males.

No consistent changes related to the administration of TNP in hematological or blood biochemical parameters or necropsy findings were found at any doses.

Repeated dose study in newborn rats (main study)

There were no deaths throughout the experimental period in males and females, even at 65.1 mg/kg per day. Yellowish fur was observed in all TNP-treated rats. A significantly lower BW (max. 7% decreased) was found in males on days 4 and 8 of the dosing period at 65.1 mg/kg per day. During the recovery-maintenance period, no dose-dependent effects on BW and food consumption were observed.

No toxicological effects of TNP on physical development, reflex ontogeny, and sexual maturation were detected at any doses in the newborn rat study.

The organ weights are summarized in Table 1. Significantly higher relative weights of the liver in males and females (13 and 12% increased, respectively) were observed at 65.1 mg/kg per day.

No consistent changes related to the administration of TNP were found in hematological or biochemical parameters, urinalysis or histopathological findings.

Repeated dose study in young rats (dose-finding study)

All male rats and one female rat at 500 mg/kg per day died by day 2 of the dosing period. No death was found at 20 and 100 mg/kg per day. Yellowish fur was observed in all TNP-treated rats. BW of males and females at 20 and 100 mg/kg per day were not significantly different from controls during the dosing period.

The results of hematological examinations are summarized in Table 2. Significantly lower values of Hb and Ht, and a higher value of Ret were detected in females at 100 mg/kg per day.

The organ weights are summarized in Table 3. At 100 mg/kg per day, a significantly higher value of relative spleen weight (14% increased) in males, and a significantly higher value of relative liver weight (18% increased) in females were observed.

Repeated dose study in young rats (main study)

There were no deaths throughout the experimental period even at 100 mg/kg per day. Yellowish fur was observed in all TNP-treated rats. A yellowish color change of urine was also found in all TNP-treated groups during the dosing period and this coloration disappeared during the recovery period. BW of males and females in the TNP-treated groups were not significantly different from controls during the dosing and recovery periods. No consistent changes in food consumption were found in the TNP-treated groups.

The results of hematological examinations are summarized in Table 2. Significantly higher values of WBC and Ret and lower values of RBC and Hb were observed in males at 100 mg/kg per day. At this dose, significantly higher values of WBC, MCV and Ret, and lower values of RBC, Hb and MCHC were also found in females.

The organ weights are summarized in Table 3. Significantly higher values of relative liver weight (12% increased) and relative spleen weight (45% increased) and significantly lower value of relative epididymides weight (21% decreased) were observed in males at 100 mg/kg per day at the end of the dosing period. A Significantly lower value of relative epididymides weight at 100 mg/kg per day was also

Table 1 Organ weights in the newborn rat study of 2,4,6-trinitrophenol

	Dose-finding study†			Main study‡			
Dose (mg/kg per day)	0	16.3	81.4	0	4.1	16.3	65.1
Males							
No. animals	4	4	3	6	6	6	6
Body weight§ (g)	48.9 ± 3.7	47.7 ± 2.6	42.3 ± 2.0*	63.4 ± 4.9	63.0 ± 2.8	63.7 ± 5.7	61.8 ± 4.8
Liver (g)	1.73 ± 0.14	1.67 ± 0.13	1.70 ± 0.13	2.69 ± 0.22	2.74 ± 0.14	2.79 ± 0.24	2.97 ± 0.38
(g/100 g BW)	(3.55 ± 0.10)	(3.49 ± 0.12)	(4.01 ± 0.13)**	(4.25 ± 0.16)	(4.35 ± 0.12)	(4.38 ± 0.08)	(4.79 ± 0.28)**
Spleen (g)	0.21 ± 0.04	0.21 ± 0.02	0.17 ± 0.01	0.34 ± 0.07	0.35 ± 0.06	0.38 ± 0.04	0.37 ± 0.06
(g/100 g BW)	(0.44 ± 0.07)	(0.45 ± 0.05)	(0.40 ± 0.03)	(0.54 ± 0.07)	(0.56 ± 0.08)	(0.60 ± 0.05)	(0.60 ± 0.05)
Kidneys (g)	0.58 ± 0.03	0.56 ± 0.04	0.43 ± 0.05**	0.74 ± 0.12	0.73 ± 0.08	0.77 ± 0.03	0.73 ± 0.12
(g/100 g BW)	(1.18 ± 0.04)	(1.17 ± 0.05)	(1.02 ± 0.08)**	(1.16 ± 0.12)	(1.16 ± 0.09)	(1.21 ± 0.10)	(1.18 ± 0.12)
Epididymides (mg)	–	–	–	57.6 ± 4.6	55.4 ± 6.0	57.6 ± 7.3	50.3 ± 3.7
(mg/100 g BW)	–	–	–	(91.1 ± 6.9)	(87.9 ± 7.2)	(91.3 ± 16.4)	(81.9 ± 7.9)
Testes (mg)	–	–	–	326 ± 47	302 ± 27	319 ± 22	295 ± 20
(mg/100 g BW)	–	–	–	(513 ± 54)	(479 ± 26)	(504 ± 44)	(478 ± 27)
Females							
No. animals	4	4	2	6	6	6	6
Body weight§ (g)	45.2 ± 2.2	47.5 ± 3.1	38.6	59.0 ± 3.3	59.6 ± 2.3	57.0 ± 4.6	58.8 ± 5.3
Liver (g)	1.57 ± 0.08	1.72 ± 0.09	1.64	2.46 ± 0.22	2.44 ± 0.24	2.33 ± 0.25	2.75 ± 0.28
(g/100 g BW)	(3.48 ± 0.25)	(3.62 ± 0.10)	(4.23)	(4.18 ± 0.35)	(4.09 ± 0.29)	(4.09 ± 0.19)	(4.67 ± 0.19)*
Spleen (g)	0.20 ± 0.03	0.20 ± 0.04	0.17	0.32 ± 0.04	0.33 ± 0.04	0.29 ± 0.05	0.37 ± 0.05
(g/100 g BW)	(0.43 ± 0.04)	(0.43 ± 0.06)	(0.44)	(0.54 ± 0.05)	(0.55 ± 0.07)	(0.51 ± 0.08)	(0.62 ± 0.03)
Kidneys (g)	0.55 ± 0.02	0.57 ± 0.05	0.43	0.69 ± 0.05	0.69 ± 0.06	0.66 ± 0.06	0.70 ± 0.05
(g/100 g BW)	(1.22 ± 0.06)	(1.20 ± 0.06)	(1.12)	(1.17 ± 0.09)	(1.16 ± 0.08)	(1.16 ± 0.10)	(1.20 ± 0.06)

†Rats were killed on postnatal day (PND) 18; ‡rats were killed on PND 22; §body weight (BW) after overnight starvation follow the last dosing. Values are given as the mean ± SD. *$P < 0.05$ and **$P < 0.01$ indicate significantly different from control group. –, no data.

Table 2 Hematological parameters in the young rat study of 2,4,6-trinitrophenol

	Dose-finding study†			Main study‡			
Dose (mg/kg per day)	0	20	100	0	4	20	100
Males							
No. animals	3	3	3	6	6	6	6
WBC ($\times 10^2/\mu L$)	117 ± 26	94 ± 20	108 ± 21	93 ± 14	98 ± 14	112 ± 22	146 ± 38**
RBC ($\times 10^4/\mu L$)	682 ± 13	651 ± 24	646 ± 32	720 ± 32	720 ± 13	739 ± 34	661 ± 52*
Hb (g/dL)	14.0 ± 0.6	13.8 ± 0.2	13.8 ± 0.6	14.3 ± 0.3	14.6 ± 0.5	14.8 ± 0.7	13.4 ± 0.7*
Ht (%)	40.9 ± 1.4	41.3 ± 1.5	40.9 ± 2.7	40.9 ± 1.0	41.5 ± 1.8	42.6 ± 1.4	39.1 ± 2.2
MCV (fL)	60.0 ± 3.1	63.4 ± 1.1	63.3 ± 1.7	56.8 ± 1.6	57.7 ± 2.3	57.8 ± 2.3	59.3 ± 2.7
MCHC (%)	34.2 ± 0.3	33.5 ± 1.0	33.7 ± 0.9	35.0 ± 0.7	35.2 ± 0.6	34.8 ± 0.6	34.1 ± 0.5
Ret (‰)	59.8 ± 5.6	61.1 ± 3.7	72.6 ± 8.2	31.4 ± 1.4	29.8 ± 4.1	31.6 ± 3.8	54.7 ± 7.6**
Females							
No. animals	3	3	3	6	6	6	6
WBC ($\times 10^2/\mu L$)	82 ± 7	70 ± 12	98 ± 31	67 ± 18	79 ± 27	73 ± 15	123 ± 33**
RBC ($\times 10^4/\mu L$)	711 ± 6	690 ± 31	639 ± 47	706 ± 30	711 ± 47	713 ± 41	608 ± 19**
Hb (g/dL)	14.6 ± 0.1	14.5 ± 0.3	13.5 ± 0.7*	14.2 ± 0.5	14.3 ± 0.5	14.3 ± 0.6	12.6 ± 0.3**
Ht (%)	42.4 ± 0.3	41.4 ± 0.6	38.5 ± 1.7**	39.3 ± 1.2	40.3 ± 1.9	40.3 ± 1.8	37.3 ± 0.9
MCV (fL)	59.6 ± 0.8	60.0 ± 3.6	60.3 ± 1.8	55.8 ± 0.9	56.9 ± 3.4	56.6 ± 1.7	61.4 ± 2.4**
MCHC (%)	34.5 ± 0.4	35.2 ± 0.3	35.0 ± 0.3	36.2 ± 0.9	35.6 ± 0.6	35.6 ± 0.7	33.9 ± 0.3**
Ret (‰)	37.6 ± 1.5	39.6 ± 6.9	56.3 ± 3.6**	25.5 ± 4.6	25.2 ± 1.0	24.1 ± 3.3	65.5 ± 5.9*

†Rats were killed at 7 weeks of age; ‡rats were killed at 9 weeks of age. Values are given as the mean ± SD. *$P < 0.05$ and **$P < 0.01$ indicate significantly different from control group. Hb, hemoglobin; Ht, hematocrit; MCHC, mean corpuscular hemoglobin concentration; MCV, mean corpuscular volume; RBC, red blood cell count; Ret, reticulocyte ratio; WBC, white blood cell count.

Table 3 Organ weights in the young rat study of 2,4,6-trinitrophenol

Dose	Dose-finding study†			Main study‡				Main study (at the end of recovery period)§	
(mg/kg per day)	0	20	100	0	4	20	100	0	100
Males									
No. animals	3	3	3	6	6	6	6	6	6
Body weight¶ (g)	267 ± 15	257 ± 7	276 ± 9	374 ± 12	380 ± 31	384 ± 35	367 ± 27	449 ± 20	529 ± 43
Liver (g)	10.8 ± 0.4	10.9 ± 0.7	12.2 ± 0.2*	14.2 ± 1.3	14.0 ± 0.9	14.4 ± 1.8	15.6 ± 1.1	15.5 ± 1.1	14.8 ± 2.2
(g/100 g BW)	(4.04 ± 0.12)	(4.26 ± 0.39)	(4.43 ± 0.17)	(3.79 ± 0.31)	(3.69 ± 0.19)	(3.73 ± 0.23)	(4.24 ± 0.24)*	(3.46 ± 0.22)	(3.45 ± 0.20)
Spleen (g)	0.77 ± 0.10	0.75 ± 0.03	0.91 ± 0.07	0.82 ± 0.08	0.76 ± 0.08	0.89 ± 0.19	1.18 ± 0.16**	0.86 ± 0.09	0.84 ± 0.07
(g/100 g BW)	(0.29 ± 0.03)	(0.29 ± 0.02)	(0.33 ± 0.02)*	(0.22 ± 0.02)	(0.20 ± 0.02)	(0.23 ± 0.03)	(0.32 ± 0.03)**	(0.19 ± 0.02)	(0.20 ± 0.01)
Kidneys (g)	2.29 ± 0.25	2.12 ± 0.16	2.39 ± 0.12	2.62 ± 0.13	2.57 ± 0.13	2.81 ± 0.33	2.72 ± 0.13	2.85 ± 0.23	2.92 ± 0.31
(g/100 g BW)	(0.86 ± 0.06)	(0.83 ± 0.04)	(0.87 ± 0.02)	(0.70 ± 0.03)	(0.68 ± 0.05)	(0.73 ± 0.06)	(0.74 ± 0.03)	(0.64 ± 0.05)	(0.68 ± 0.04)
Testes (g)	–	–	–	3.08 ± 0.32	3.09 ± 0.19	3.13 ± 0.25	3.29 ± 0.35	3.30 ± 0.09	2.64 ± 1.07
(g/100 g BW)	–	–	–	(0.82 ± 0.09)	(0.82 ± 0.06)	(0.82 ± 0.05)	(0.90 ± 0.05)	(0.74 ± 0.03)	(0.61 ± 0.22)
Epididymides (g)	–	–	–	0.82 ± 0.06	0.78 ± 0.06	0.78 ± 0.07	0.63 ± 0.10**	1.10 ± 0.07	0.82 ± 0.11**
(g/100 g BW)	–	–	–	(0.22 ± 0.02)	(0.21 ± 0.02)	(0.20 ± 0.01)	(0.17 ± 0.03)**	(0.24 ± 0.01)	(0.20 ± 0.03)**
Female									
No. animals	3	3	3	6	6	6	6	6	6
Body weight¶ (g)	165 ± 9	172 ± 4	175 ± 8	242 ± 19	241 ± 17	237 ± 29	233 ± 14	283 ± 18	270 ± 19
Liver (g)	6.4 ± 0.8	6.7 ± 0.1	8.0 ± 0.6*	8.2 ± 0.7	8.0 ± 0.8	8.2 ± 1.5	9.7 ± 1.2	9.3 ± 0.7	9.3 ± 1.1
(g/100 g BW)	(3.85 ± 0.28)	(3.90 ± 0.07)	(4.54 ± 0.23)*	(3.38 ± 0.11)	(3.32 ± 0.15)	(3.45 ± 0.19)	(4.16 ± 0.27)**	(3.27 ± 0.15)	(3.43 ± 0.27)
Spleen (g)	0.49 ± 0.13	0.45 ± 0.13	0.56 ± 0.05	0.51 ± 0.08	0.58 ± 0.05	0.54 ± 0.08	0.98 ± 0.12**	0.60 ± 0.10	0.63 ± 0.09
(g/100 g BW)	(0.30 ± 0.06)	(0.26 ± 0.08)	(0.32 ± 0.01)	(0.21 ± 0.04)	(0.24 ± 0.02)	(0.23 ± 0.20)	(0.42 ± 0.05)**	(0.21 ± 0.02)	(0.23 ± 0.02)
Kidneys (g)	1.40 ± 0.03	1.45 ± 0.13	1.52 ± 0.17	1.77 ± 0.16	1.73 ± 0.20	1.67 ± 0.20	1.86 ± 0.17	1.82 ± 0.12	1.86 ± 0.10
(g/100 g BW)	(0.85 ± 0.03)	(0.84 ± 0.07)	(0.87 ± 0.11)	(0.74 ± 0.07)	(0.71 ± 0.04)	(0.71 ± 0.05)	(0.80 ± 0.06)	(0.65 ± 0.06)	(0.69 ± 0.06)

†Rats were killed at 7 weeks of age; ‡rats were killed at 9 weeks of age; §rats were killed at 11 weeks of age; ¶body weight (BW) after overnight starvation following the last dosing. Values are given as the mean ± SD. *$P < 0.05$ and **$P < 0.01$ indicate significantly different from control group. –, no data.

noted at the end of the recovery period. At this dose in females, significantly higher values of relative liver weight (23% increased) and relative spleen weight (100% increased) were noted. No other changes related to the administration of TNP were found.

At the end of the dosing period, enlargement of the spleen and erosion or ulcers in the cecum were observed in males and females at 100 mg/kg per day. Small testes were found at 100 mg/kg per day at the end of the recovery period.

The histopathological findings are summarized in Table 4. Significant changes were noted at 100 mg/kg per day. Spleens with the development of a germinal center and extramedullary hematopoiesis were observed in males and females at 100 mg/kg per day at the end of the dosing period. Hemosiderin deposition in the spleen was found in males and females at 100 mg/kg per day at the end of the dosing and recovery periods. Centrilobular hypertrophy of hepatocytes in the liver and ulcers in the cecum were observed in males and females at 100 mg/kg per day at the end of the dosing period. Testes with diffuse atrophy of seminiferous tubules were noted at 100 mg/kg per day at the end of the dosing period, and severe atrophy was observed at the end of the recovery period. A decreased number of sperm and lumen with cell debris were observed in the epididymides at 100 mg/kg per day at the end of the dosing and recovery periods.

There were no consistent changes related to the administration of TNP in biochemical parameters for blood or urine.

DISCUSSION

In the present study, we re-evaluated the toxicity of TNP in young rats in terms of the NOAEL and toxicity profile, and determined the toxicity of this chemical in newborn rats, then compared the toxicity in newborn and young rats. We showed here that TNP had a markedly different toxicity profile between newborn and young rats.

As for the yellowish fur in all newborn and young rats treated with TNP, their hair roots and skin showed no anomalies therefore it does not seem to be an adverse effect of TNP.

In the newborn rat study, the major toxicity was death and low BW without any other toxicologically significant changes at 81.4 mg/kg per day in the dose-finding study. Deaths occurred in days 3–7 after dosing onset. At the lower dose, 65.1 mg/kg per day in the main study, a slightly low BW in males was observed only at 4 and 8 days after dosing onset. This slight and transient loss of BW might be accepted as having no toxicological significance in general, but we considered it to be closely related to the death that occurred at the higher dose, 81.4 mg/kg per day, because death and low BW were observed on the same days after dosing onset (late in the first week). Slight changes in relative liver and kidney weights were observed but not considered toxicologically significant because there were no changes in biochemical and urinary parameters, or histopathological findings. Based on low BW at 65.1 mg/kg per day in males, the NOAEL for newborn rats was considered 16.3 mg/kg per day.

In the MHLW (2001) report, the NOEL was concluded 4 mg/kg per day based on yellowish fur and decreased level of urine potassium in young rats. The major adverse effects of TNP were hemolytic anemia and testicular toxicity without death or changes of BW at 100 mg/kg per day in the main study with young rats. No toxic effects were detected at 20 mg/kg per day or less after administration of TNP in the dose-finding or main study with young rats. Based on these findings, we re-evaluated that the NOAEL for young rats was considered 20 mg/kg per day.

TNP, at 81.4 mg/kg per day or more, caused behavioral changes in the newborn rat study but not in the young rat study at 100 mg/kg per day. The immature blood–brain barrier in newborn rats may explain these phenomena. The diffusional resistance is primarily the result of tight junctions between endothelial cells, the absence of pores within the cells and a thicker, more developed basement membrane surrounding each cell (Reese & Karnovsky 1967; Scheuplein *et al.* 2002). In rats, capillary diffusion decreases during postnatal weeks 3–4 (Bär & Wolff 1972).

Histopathological and hematological examinations revealed hemolytic anemia as evidenced by reductions of RBC and Hb and hemosiderin deposition and extramedullary hematopoiesis in spleen at 100 mg/kg per day in the young rat study, but not in the newborn rat study at 81.4 mg/kg per day. Hemolytic anemia can be induced by various kinds of medicines and chemicals including some aromatic amines due to oxidation (Bloom & Brandt 2001). TNP may not be the causal substance because it occurred in young rats but not in newborn rats whose metabolic capacity is immature, such as lower total cytochrome P-450 levels (Imaoka *et al.* 1991). Thus, TNP metabolites might be the cause. As for absorption and excretion of TNP in rats, Wyman *et al.* (1992) reported that fasted rats would absorb about 60% of orally treated TNP in 24 h and the main metabolite was picramic acid following oral dosing in rats. Picramic acid, a type of aromatic amine, would be the most likely candidate, although there is no evidence of hemolytic anemia caused by picramic acid. The information together suggests that the absence of hemolytic anemia in newborn rats may be due to insufficient amounts of picramic acid produced as a metabolite of TNP.

As for the testicular toxicity, degenerating primary spermatocytes and alterations in Sertoli cells were caused by di(2-ethylhexyl) phthalate in 5-week-old, but not 3-week-old, rats (Sjöberg *et al.* 1985). TNP also had toxic effects on the testes and epididymides in young rats, but not in

Table 4 Histopathological findings at the end of dosing and recovery periods in the young rat main study of 2,4,6-trinitrophenol

		Dosing period†					Recovery period‡		
Dose (mg/kg per day)		0	4	20	100		0	100	
Males									
No. animals examined		6	6	6	6		6	6	
Spleen									
Development, germinal center	+	0	0	0	5	*	0	0	
Extramedullary hematopoiesis, erythrocyte	+	0	0	0	6	**	0	0	
Hemosiderin deposition	Total	0	0	0	4		0	6	
	+	0	0	0	3		0	6	**
	++	0	0	0	1		0	0	
Cecum									
Ulcer	Total	0	0	0	4		0	0	
	+	0	0	0	1		0	0	
	++	0	0	0	2		0	0	
	+++	0	0	0	1		0	0	
Liver									
Hypertrophy, hepatocytes, centrilobular	+	0	0	0	4		0	0	
Testis									
Atrophy, seminiferous tubules, diffuse	Total	0	0	0	6		0	5	
	+	0	0	0	6	**	0	2	*
	++	0	0	0	0		0	3	
Epididymis									
Cell debris, lumen	Total	0	0	0	4		0	1	
	+	0	0	0	3		0	1	
	++	0	0	0	1		0	0	
Decrease in sperm	Total	0	0	0	6		0	3	
	+	0	0	0	5		0	0	
	++	0	0	0	1	**	0	1	
	+++	0	0	0	0		0	2	
Females									
No. animals examined		6	6	6	6		6	6	
Spleen									
Development, germinal center	+	0	0	0	5	*	0	0	
Extramedullary hematopoiesis, erythrocyte	+	0	0	0	6	**	0	0	
Hemosiderin deposition	Total	0	0	0	6		0	6	
	+	0	0	0	3	**	0	6	**
	++	0	0	0	3		0	0	
Cecum									
Ulcer	++	0	0	0	3		0	0	
Liver									
Hypertrophy, hepatocytes, centrilobular	+	0	0	0	3		0	0	

Grade sign: +, mild; ++, moderate; +++, marked. †Rats were killed at 7 weeks of age; ‡rats were killed at 9 weeks of age. *$P < 0.05$ and **$P < 0.01$ indicate significantly different from control group.

newborn rats. The Sertoli cells play an important role in the establishment and maintenance of the specific microenvironment of the adluminal compartment of the seminiferous epithelium and this is a prerequisite for normal spermatogenesis (Sjöberg *et al.* 1986). In rats, Sertoli cells proliferate rapidly from day 19 of gestation to PND 15, then slow down and cease multiplying on approximately PND 20 (Orth 1982, Orth 1984; Toppari *et al.* 1996). The dosing periods were PND 4–21 and postnatal weeks 5–8 in the newborn and young rat studies, respectively. Therefore, TNP seems unlikely to affect the differentiation and proliferation of Sertoli cells, and seems likely to affect the maturation of spermatids, although it remains to be elucidated whether this is a direct effect of TNP or some kind of TNP metabolite.

In conclusion, in the newborn rat study, the NOAEL for TNP were 16.3 mg/kg per day, low BW at 65.1 mg/kg per day or more, and death at 81.4 mg/kg per day were observed. In the young rat study, the NOAEL for TNP were 20 mg/kg per day and hemolytic anemia and testicular toxicity were found at 100 mg/kg per day.

ACKNOWLEDGMENTS

The authors gratefully acknowledge the financial support of the Office of Chemical Safety, Pharmaceutical and Medical Safety Bureau, Ministry of Health, Labor and Welfare, Japan.

REFERENCES

Bär TH, Wolff JR (1972) The formation of the capillary basement membranes during internal vascularization of the rat's cerebral cortex. *Z Zellforsch* **133**: 231–248.

Bloom JC, Brandt JT (2001) Toxic responses of the blood. In: Klaassen CD (ed.) *Casarett and Doull's Toxicology: The Basic Science of Poisons*, 6th edn. McGraw-Hill, New York, p397.

Fomon SJ, Haschke F, Ziegler EE, Nelson SE (1982) Body composition of reference children from birth to age 10 years. *Am J Clin Nutr* **35**: 1169–1175.

Fukuda N, Ito Y, Yamaguchi M *et al.* (2004) Unexpected nephrotoxicity induced by tetrabromobisophenol A in newborn rats. *Toxicol Lett* **150**: 145–155.

Health Council of the Netherlands (2002) *Health-based Reassessment of Administrative Occupational Exposure Limits – Picric Acid.* Committee on Updating of Occupational Exposure Limits, a committee of the Health Council of the Netherlands. Health Council of the Netherlands, the Netherlands.

Imaoka S, Fujita S, Funae Y (1991) Age-dependent expression of cytochrome P-450s in rat liver. *Biochim Biophys Acta* **1097**: 187–192.

Kearns GL, Reed MD (1989) Clinical pharmacokinetics in infants and children: A reappraisal. *Clin Pharmacokinet* **17**: 29–67.

Koizumi M, Nishimura N, Enami T *et al.* (2002) Comparative toxicity study of 3-aminophenol in newborn and young rats. *J Toxicol Sci* **27**: 411–421.

Koizumi M, Noda A, Ito Y *et al.* (2003) Higher susceptibility of newborn than young rats to 3-methylphenol. *J Toxicol Sci* **28**: 59–70.

Koizumi M, Yamamoto Y, Ito Y *et al.* (2001) Comparative study of toxicity of 4-nitrophenol and 2,4-dinitrophenol in newborn and young rats. *J Toxicol Sci* **26** (5): 299–311.

Ministry of Health and Welfare Japan (1988) *Standard Concerning Testing Facility Provided in Article 4 of Order Prescribing Test Items Relating to New Chemical Substances and Toxicity Research of Designated Chemical Substances.* Planning and Coordination Bureau, Environment Agency, No. 39, Environmental Health Bureau, Ministry of Health and Welfare, No. 229. Basic Industries Bureau, Ministry of International Trade and Industry, No. 85, March 31, 1984, and amendments, November 18, 1988. MHW, Japan.

Ministry of Health, Labour, Welfare Japan (2001) 2,4,6-trinitrophenol (88–89–1). *Toxicity Testing Reports Environmental Chemicals.* MHLW, Japan, 8: 238–243.

National Research Council USA (1993) *Pesticides in the Diets of Infants and Children.* NRC, USA. National Academy Press, Washington DC.

Organisation for Economic Co-operation and Development (1981) *OECD Principles of Good Laboratory Practice.* OECD, Paris.

Organisation for Economic Co-operation and Development (1997) *OECD Principles of Good Laboratory Practice* (as revised in 1997). OECD, Paris.

Orth JM (1982) Proliferation of Sertoli cells in fetal and postnatal rats: A quantitative autoradiographic study. *Anat Rec* **203**: 485–492.

Orth JM (1984) The role of follicle-stimulating hormone in controlling Sertoli cell proliferation in testes of fetal rats. *Endocrinology* **115**: 1248–1255.

Reese TS, Karnovsky MJ (1967) Fine structural localization of a blood–brain barrier to exogenous peroxidase. *J Cell Biol* **34**: 207–217.

Scheuplein R, Charnley G, Dourson M (2002) Differential sensitivity of children and adults to chemical toxicity. *Regul Toxicol Pharmacol* **35**: 429–447.

Schwenk M, Gundert-Remy U, Heinemeyer G *et al.* (2002) Children as a sensitive subgroup and their role in regulatory toxicology: DGPT workshop report. *Arch Toxicol* **77**: 2–6.

Sjöberg POJ, Bondesson UG, Sedin EG, Gustafsson JP (1985) Exposure of newborn infants to plasticizers: Plasma levels of di-(2-ethylhexyl) phthalate and mono-

(2-ethylhexyl) phthalate during exchange transfusion. *Transfusion* **25**: 424–428.

Sjöberg P, Lindqvist NG, Plöen L (1986) Age-dependent response of the rat testes to di-(2-ethylhexyl) phthalate. *Environ Health Perspect* **65**: 237–242.

Toppari J, Larsen JC, Christiansen P *et al.* (1996) Male reproductive health and environmental xenoestrogens. *Environ Health Perspect* **104** (Suppl. 4): 741–803.

US Environmental Protection Agency (1998) *The EPA Children's Environmental Health Yearbook.* US EPA, Washington DC.

World Health Organization (1986) *Principles for Evaluating Risks from Chemicals during Infancy and Early Childhood: The Need for a Special Approach.* WHO, Geneva.

Wyman JF, Serve MP, Hobson DW, Lee LH, Uddin DE (1992) Acute toxicity, distribution, and metabolism of 2,4,6-trinitrophenol (picric acid) in Fischer 344 rats. *J Toxicol Environ Health* **37**: 313–327.

Differential contributions of Mesp1 and Mesp2 to the epithelialization and rostro-caudal patterning of somites

Yu Takahashi[1,*], Satoshi Kitajima[1], Tohru Inoue[1], Jun Kanno[1] and Yumiko Saga[2,*]

[1]Cellular & Molecular Toxicology Division, National Institute of Health Sciences, 1-18-1 Kamiyoga, Setagayaku, Tokyo 158-8501, Japan
[2]Division of Mammalian Development, National Institute of Genetics, Yata 1111, Mishima 411-8540, Japan
*Authors for correspondence (e-mail: yutak@nihs.go.jp and ysaga@lab.nig.ac.jp)

Accepted 29 November 2004

Development 132, 787-796
Published by The Company of Biologists 2005
doi:10.1242/dev.01597

Summary

Mesp1 and Mesp2 are homologous basic helix-loop-helix (bHLH) transcription factors that are co-expressed in the anterior presomitic mesoderm (PSM) just prior to somite formation. Analysis of possible functional redundancy of Mesp1 and Mesp2 has been prevented by the early developmental arrest of Mesp1/Mesp2 double-null embryos. Here we performed chimera analysis, using either Mesp2-null cells or Mesp1/Mesp2 double-null cells, to clarify (1) possible functional redundancy and the relative contributions of both Mesp1 and Mesp2 to somitogenesis and (2) the level of cell autonomy of Mesp functions for several aspects of somitogenesis. Both Mesp2-null and Mesp1/Mesp2 double-null cells failed to form initial segment borders or to acquire rostral properties, confirming that the contribution of Mesp1 is minor during these events. By contrast, Mesp1/Mesp2 double-null cells contributed to neither epithelial somite nor dermomyotome formation, whereas Mesp2-null cells partially contributed to incomplete somites and the dermomyotome. This indicates that Mesp1 has a significant role in the epithelialization of somitic mesoderm. We found that the roles of the Mesp genes in epithelialization and in the establishment of rostral properties are cell autonomous. However, we also show that epithelial somite formation, with normal rostro-caudal patterning, by wild-type cells was severely disrupted by the presence of Mesp mutant cells, demonstrating non-cell autonomous effects and supporting our previous hypothesis that Mesp2 is responsible for the rostro-caudal patterning process itself in the anterior PSM, via cellular interaction.

Key words: Somitogenesis, Epithelial-mesenchymal conversion, Mesp2, Chimera analysis, Mouse

Introduction

Somitogenesis is not only an attractive example of metameric pattern formation but is also a good model system for the study of morphogenesis, particularly epithelial-mesenchymal interconversion in vertebrate embryos (Gossler and Hrabe de Angelis, 1997; Pourquié, 2001). The primitive streak, or tailbud mesenchyme, supplies the unsegmented paraxial mesoderm, known as presomitic mesoderm (PSM). Mesenchymal cells in the PSM undergo mesenchymal-epithelial conversion to form epithelial somites in a spatially and temporally coordinated manner. Somites then differentiate, in accordance with environmental cues from the surrounding tissues, into dorsal epithelial dermomyotome and ventral mesenchymal sclerotome (Borycki and Emerson, 2000; Fan and Tessier Lavigne, 1994). Hence, the series of events that occur during somitogenesis provide a valuable example of epithelial-mesenchymal conversion. The dermomyotome gives rise to both dermis and skeletal muscle, whereas the sclerotome forms cartilage and bone in both the vertebrae and the ribs. Each somite is subdivided into two compartments, the rostral (anterior) and caudal (posterior) halves. This rostro-caudal polarity appears to be established just prior to somite formation (Saga and Takeda, 2001).

Mesp1 and Mesp2 are closely related members of the basic helix-loop-helix (bHLH) family of transcription factors but share significant sequence homology only in their bHLH regions (Saga et al., 1996; Saga et al., 1997). During development of the mouse embryo, both *Mesp1* and *Mesp2* are specifically expressed in the early mesoderm just after gastrulation and in the paraxial mesoderm during somitogenesis. Mesp1/Mesp2 double-null embryos show defects in early mesodermal migration and thus fail to form most of the embryonic mesoderm, leading to developmental arrest (Kitajima et al., 2000). Mesp1-null embryos exhibit defects in single heart tube formation, due to a delay in mesodermal migration, but survive to the somitogenesis stage (Saga et al., 1999), suggesting that there is some functional redundancy, i.e. compensatory functions of Mesp2 in early mesoderm. During somitogenesis, both *Mesp1* and *Mesp2* are expressed in the anterior PSM just prior to somite formation. Although we have shown that Mesp2, but not Mesp1, is essential for somite formation and the rostro-caudal patterning of somites (Saga et al., 1997), a possible functional redundancy between Mesp1 and Mesp2 has not yet been clearly established.

To further clarify the contributions of Mesp1 and Mesp2 to somitogenesis, analysis of Mesp1/Mesp2 double-null embryos

is necessary, but because of the early mesodermal defects already described, these knockout embryos lack a paraxial mesoderm, which prevents any analysis of somitogenesis. We therefore adopted a strategy that utilized chimera analysis. As we have reported previously, the early embryonic lethality of a Mesp1/Mesp2 double knockout is rescued by the presence of wild-type cells in a chimeric embryo, but the double-null cells cannot contribute to the cardiac mesoderm (Kitajima et al., 2000). This analysis, however, focused only on early heart morphogenesis and did not investigate the behavior of Mesp1/Mesp2 double-null cells in somitogenesis. In this report, we focus upon somitogenesis and compare two types of chimeras using either Mesp1/Mesp2 double-null cells or Mesp2-null cells to investigate Mesp1 function during somitogenesis.

Another purpose of our chimera experiments was to elucidate the cell autonomy of Mesp functions. In the process of somite formation, mesenchymal cells in the PSM initially undergo epithelialization at the future segment boundary, independently of the already epithelialized dorsal or ventral margin of the PSM (Sato et al., 2002). Epithelial somite formation is disrupted in the Mesp2-null embryo, indicating that Mesp2 is required for epithelialization at the segment boundary. Although Mesp products are nuclear transcription factors and their primary functions must therefore be cell autonomous (transcriptional control of target genes), it is possible that the roles of Mesp2 in epithelialization are mediated by the non-cell autonomous effects of target genes. We therefore asked whether the defects in Mesp2-null cells during epithelialization could be rescued by the presence of surrounding wild-type cells. Additionally, we would expect to find that the role of Mesp2 in establishing rostro-caudal polarity is rescued in a similar way.

Our analysis suggests that Mesp1 and Mesp2 have redundant functions and are both cell-autonomously involved in the epithelialization of somitic mesoderm. In addition, our results highlight some non-cell autonomous effect of Mesp2-null and Mesp1/Mesp2-null cells.

Materials and methods

Generation of chimeric embryos

As described previously (Kitajima et al., 2000), chimeric embryos were generated by aggregating 8-cell embryos of wild-type mice (ICR) with those of mutant mice that were genetically marked with the *ROSA26* transgene (Zambrowicz et al., 1997). Mesp1/Mesp2 double-null embryos were generated by crossing *wko-del (+/–)* and *Mesp1(+/–)/Mesp2(+/cre)* mice as described previously (Kitajima et al., 2000). This strategy enables us to distinguish chimeric embryos derived from homozygous embryos, which have two different mutant alleles, from those derived from heterozygous embryos. Likewise, Mesp2-null embryos were generated by crossing *P2v1(+/–)* mice (Saga et al., 1997) and *P2GFP (+/gfp)* mice (Y.S. and S.K., unpublished) that were also labeled with the *ROSA26* locus. The genotype of the chimeric embryos was determined by PCR using yolk sac DNA.

Histology, histochemistry and gene expression analysis

The chimeric embryos were fixed at 11 days postcoitum (dpc) and stained in X-gal solution for the detection of β-galactosidase activity, as described previously (Saga et al., 1999). For histology, samples stained by X-gal were postfixed with 4% paraformaldehyde, dehydrated in an ethanol series, embedded in plastic resin (Technovit 8100, Heraeus Kulzer) and sectioned at 3 μm. The methods used for gene expression analysis by in-situ hybridization of whole-mount samples and frozen sections and skeletal preparation by Alcian Blue/Alizarin Red staining were described previously (Saga et al., 1997; Takahashi et al., 2000). Probes for in-situ hybridization for *Uncx4.1* (Mansouri et al., 1997; Neidhardt et al., 1997), *Delta-like 1 (Dll1)* (Bettenhausen et al., 1995) and *Paraxis* (Burgess et al., 1995) were kindly provided by Drs Peter Gruss, Achim Gossler and Alan Rawls, respectively. A probe for *EphA4* (Nieto et al., 1992) was cloned by PCR. For detection of actin filaments, frozen sections were stained with AlexaFluor 488-conjugated phalloidin (Molecular Probes) according to the manufacturer's protocol.

Results

Possible functional redundancy and different contributions of Mesp1 and Mesp2 in somitogenesis

During somitogenesis, both *Mesp1* and *Mesp2* are expressed in the anterior PSM just prior to somite formation and their expression domains overlap (Fig. 1A). Mesp1-null embryos form morphologically normal somites and show normal rostro-caudal patterning within each somite (Fig. 1B,E-H), indicating that Mesp1 is not essential for somitogenesis. By contrast, Mesp2 is essential for both the formation and rostro-caudal patterning of somites, as Mesp2-null embryos have no epithelial somites and lose rostral half properties, resulting in caudalization of the entire somitic mesoderm (Saga et al., 1997) (Fig. 1C,D).

Although somite formation and rostro-caudal patterning is disrupted in the Mesp2-null embryo, histological differentiation into dermomyotome and sclerotome is not affected. It is noteworthy that the Mesp2-null embryo still forms disorganized dermomyotomes without forming epithelial somites (Saga et al., 1997). As *Mesp1* is expressed at normal levels in the PSM of Mesp2-null embryos (Fig. 1C,D), it is possible that Mesp1 functions to rescue some aspects of somitogenesis in the Mesp2-null embryo. In order to further clarify the contributions of both Mesp1 and Mesp2 during somitogenesis, we therefore generated chimeric embryos with either Mesp2-null cells or Mesp1/Mesp2 double-null cells and compared the behavior of mutant cells during somitogenesis (Fig. 2).

Mesp2-null cells tend to be eliminated from the epithelial somite and the dermomyotome, but can partially contribute to both of these structures

We first generated Mesp2-null chimeric embryos (*Mesp2*$^{+/-}$ with *Rosa26*: wild) to analyze cell autonomy of Mesp2 function during somitogenesis. The control chimeric embryo (*Mesp2*$^{+/-}$ with *Rosa26*: wild) showed normal somitogenesis and a random distribution of X-gal stained cells (Fig. 3A). The Mesp2-null chimeric embryos formed abnormal somites that exhibited incomplete segmentation (Fig. 3B), but histological differentiation of dermomyotome and sclerotome was observed. Within the incomplete somite, X-gal-stained Mesp2-null cells were mainly localized in the rostral and central regions, surrounded by wild-type cells at the dorsal, ventral and caudal sides (Fig. 3B). The surrounding wild-type cells, however, did not form an integrated epithelial sheet, but consisted of several epithelial cell clusters. Such trends were more obviously observed in other sections, where wild-type cells were found to form multiple small epithelial clusters (Fig.

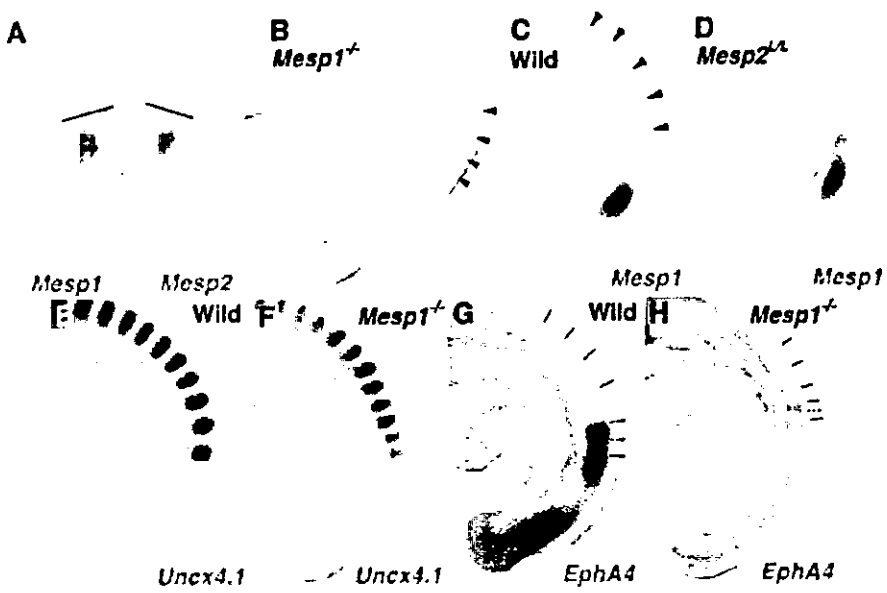

Fig. 1. *Mesp1* and *Mesp2* are co-expressed in the anterior PSM but have differing roles in somitogenesis. (A) Overlapping expression of *Mesp1* and *Mesp2* is revealed by in-situ hybridization using the left and right halves of the same embryo. The lines show most recently formed somite boundaries. (B-C) A Mesp1-null embryo (B) shows the same normal somite formation as a wild-type embryo (C). Arrowheads indicate somite boundaries. (D) In Mesp2-null embryos, no somite formation is observed but *Mesp1* is expressed at comparable levels to wild type, although its expression is anteriorly extended and blurred. (E-H) Mesp1-null embryos show normal rostro-caudal patterning of somites. (E,F) Expression of a caudal half marker, *Uncx4.1*. (G,H) Expression of a rostral half marker, *EphA4*. The lines indicate presumptive or formed somite boundaries and the dotted line indicates approximate position of somite half boundary.

3C,D). Mesp2-null cells tended to be eliminated from the epithelial clusters, although they were partially integrated into these structures (blue arrows in Fig. 3C,D). Likewise, small numbers of Mesp2-null cells were found to contribute to the dermomyotome (Fig. 3E,F). Mesp2-null cells also appeared to form the major part of the sclerotome.

Mesp2 is required for the cell-autonomous acquisition of rostral properties

We have previously demonstrated that suppression by Mesp2

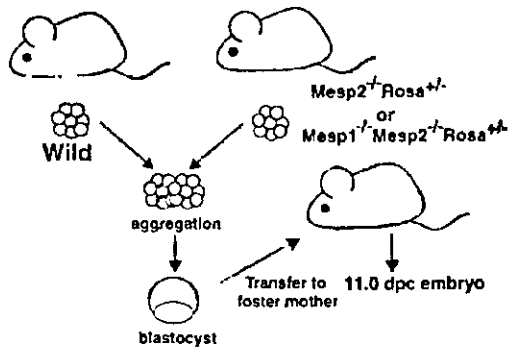

Fig. 2. Schematic representation of chimera analysis method. Either Mesp2-null or Mesp1/Mesp2 double-null embryos, genetically labeled with *Rosa* locus, were aggregated with wild-type embryos at the 8-cell stage, and the resulting chimeras were subjected to analysis at 11.0 dpc.

of the caudal genes *Dll1* and *Uncx4.1* in presumptive rostral half somites is a crucial event in the establishment of the rostro-caudal pattern of somites (Saga et al., 1997; Takahashi et al., 2000). As Mesp2-null embryos exhibit caudalization of somites, Mesp2-null cells are predicted to be unable to express rostral properties. Hence, Mesp2-null cells are expected to distribute to the caudal region of each somite where the rostro-caudal patterns are rescued by wild-type cells in a chimeric embryo. In this context, the localization of Mesp2-null cells at the rostral side was an unexpected finding. We interpret this to mean that the rostral location of Mesp2-null cells is due to a lack of epithelialization functions (see Discussion).

To examine rostro-caudal properties in Mesp2-null cells, located in the rostral side, we analyzed the expression of a caudal half marker gene, *Uncx4.1* (Mansouri et al., 1997; Neidhardt et al., 1997). Analysis of adjacent sections revealed that *lacZ*-expressing Mesp2-null cells, localized at the rostral and central portion, ectopically expressed *Uncx4.1* (Fig. 4A-D). This strongly suggests that Mesp2-null cells cannot acquire rostral properties even if surrounded by wild-type cells, and that Mesp2 function is cell-autonomously required for the acquisition of rostral properties. We also observed that the small number of Mesp2-null cells distributed mostly to the caudal end of the dermomyotome (Fig. 3E,F) and that the expression pattern of *Uncx4.1* was normal in the dermomyotome (Fig. 4E,F). In the sclerotome, *lacZ*-expressing Mesp2-null cells often distributed to the rostral side, where expression of *Uncx4.1* was abnormally elevated (Fig. 4G,H). The vertebrae of the Mesp2-null chimeric fetus showed a partial fusion of the neural arches, which was reminiscent of

Mesp2-hypomorphic fetuses (Fig. 4I,J) (Nomura-Kitabayashi et al., 2002). Fusion of proximal rib elements was also observed (Fig. 4K,L).

Mesp1/Mesp2 double-null cells cannot contribute to the formation of epithelial somites or to the dermomyotome

To address the question of whether Mesp1, in addition to Mesp2, exhibits any function during somitogenesis, we next generated Mesp1/Mesp2 double-null chimeric embryos and compared them with the Mesp2-null chimeric embryos described in the previous sections. We first performed whole-mount X-gal staining of embryos at 11 dpc. In the control chimeric embryo, the X-gal-stained Mesp1/Mesp2 double-heterozygous cells distributed randomly throughout the embryonic body, including the somite region (Fig. 5A,C). By contrast, the Mesp1/Mesp2 double-null chimeric embryo displayed a strikingly uneven pattern of cellular distribution in the somite region. The X-gal stained Mesp1/Mesp2 double-null cells were localized at the medial part of embryonic tail and were not observed in the lateral part of the somite region (Fig. 5B,D). Histological examination of parasagittal sections further revealed obvious differences in the cellular contribution to somite formation (Fig. 5E,F). In the control chimeric embryo, Mesp1/Mesp2 double-heterozygous cells distributed randomly throughout the different stages of somitogenesis (PSM, somite, dermomyotome and sclerotome: Fig. 5E). In the Mesp1/Mesp2 double-null chimeric embryo, neither the initial segment border nor epithelial somites were formed, but histologically distinguishable dermomyotome-like and sclerotome-like compartments were generated (Fig. 5F). In addition, Mesp1/Mesp2 double-null cells and wild-type cells were randomly mixed in the PSM, whereas the dermomyotome-like epithelium consisted exclusively of wild-type cells and the sclerotome-like compartment consisted mostly of Mesp1/Mesp2 double-null cells. This suggests that either Mesp1 or Mesp2 is cell-autonomously required for the formation of epithelial somite and dermomyotome. These results also indicate that PSM cells with different characteristics are rapidly sorted during somite formation.

Subsequent examination of transverse sections confirmed the elimination of Mesp1/Mesp2 double-null cells from dermomyotome (Fig. 5G,H). In the mature somite region, the wild-type dermomyotome-like epithelium was found to form the myotome (my) (Fig. 5I,J). Furthermore, the ventral part of this dermomyotome-like epithelium became mesenchymal and appeared to contribute to the dorsal sclerotome (dsc), implying that this initial dermomyotome-like epithelium actually corresponds to the epithelial somite exclusively composed of wild-type cells (Fig. 5I,J). Fluorescent phalloidin staining revealed that the apical localization of actin filaments is limited to the dorsal compartments, which are occupied by wild-type cells in the Mesp1/Mesp2 double-null chimeric embryo (Fig. 5K,L), indicating the Mesp1/Mesp2 double-null cells cannot undergo epithelialization.

It is known that the bHLH transcription factor paraxis (Tcf15 – Mouse Genome Informatics), is required for the epithelialization of somite and

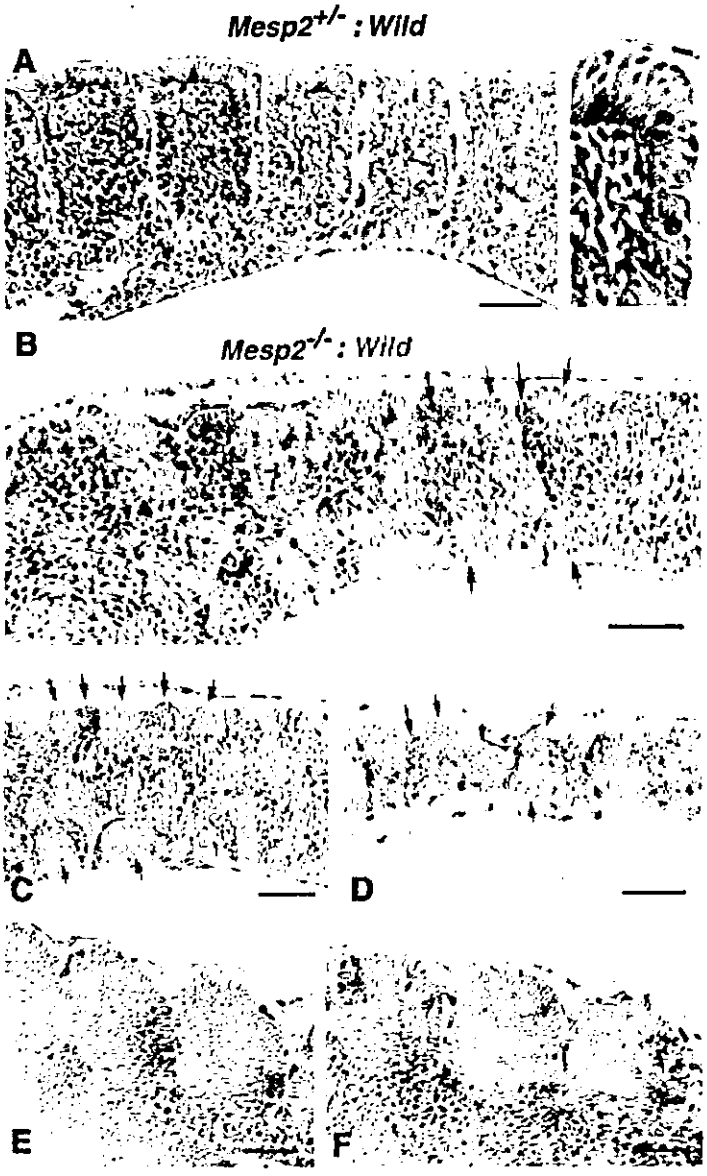

Fig. 3. Mesp2-null cells tend to be excluded from the epithelial region of the somites. (A) The control chimeric embryo undergoes normal somite formation and shows random distribution of labeled cells. The right panel is a high-power view of a somite. (B) In the Mesp2-null chimeric embryo, incompletely segmented somites are formed. Mesp2-null cells tend to be localized at the rostral and central region of these incomplete segments. Red arrows: wild-type cell clusters; blue arrows: Mesp2-null cell clusters. (C,D) Other sections indicating multiple small epithelial cell clusters (arrows). Note that Mesp2-null cells only partially contribute to the epithelial clusters (blue arrows). (E,F) A small number of Mesp2-null cells are distributed in the dermomyotome and are mostly localized at the caudal end. Scale bars: 100 μm.

dermomyotome (Burgess et al., 1995; Burgess et al., 1996). Although *Paraxis* expression is not affected in Mesp2-null embryos (data not shown), it is possible that it is influenced by the loss of both Mesp1 and Mesp2. We therefore examined the expression patterns of *Paraxis* in our Mesp1/Mesp2 double-null chimeras. In wild-type embryos *Paraxis* is initially expressed throughout the entire somite region (in both the prospective dermomyotomal and sclerotomal regions) in the anteriormost PSM and newly forming somites, and then localizes in the dermomyotomes (Burgess et al., 1995). The dorsal dermomyotomal epithelium, composed of wild-type cells, strongly expressed *Paraxis* in the chimeric embryo (Fig. 6A,B). In addition, adjacent sections revealed that *lacZ*-expressing Mesp1/Mesp2 double-null cells expressed *Paraxis* in the medial sclerotomal compartment (Fig. 6A,B, brackets). This suggests that *Paraxis* expression in the future sclerotomal region is independent of Mesp factors. However, at present we cannot exclude the possibility that the maintenance of *Paraxis* expression in the dermomyotome requires the functions of either Mesp1 or Mesp2.

Mesp1/Mesp2 double-null cells are incapable of acquiring rostral properties

To clarify the rostro-caudal properties of somites in our chimeric embryos, we examined the expression pattern of *Uncx4.1*. Control chimeric embryos exhibited a normal stripe pattern of *Uncx4.1* expression throughout the segmented somite region (Fig. 7A). By contrast, Mesp1/Mesp2 double-null chimeric embryos exhibited continuous *Uncx4.1* expression in the ventral sclerotomal region (Fig. 7B). This continuity was observed in the entire sclerotome-like compartment of the newly formed somite region and in the ventral sclerotome in the mature somite region. The caudal localization of *Uncx4.1* expression, however, was normal in the dermomyotome and the dorsal sclerotome, which consisted of wild-type cells (Fig. 5), even in Mesp1/Mesp2 double-null chimeras. This suggests that, like Mesp2-null cells, Mesp1/Mesp2 double-null cells are incapable of acquiring rostral properties. Since the mesoderm of Mesp1/Mesp2 double-null embryos lacks the expression of the major markers of paraxial mesoderm (Kitajima et al., 2000), and Mesp1/Mesp2 double-null cells do not exhibit histological features characteristic of epithelial somites in our current study, it is possible that Mesp1/Mesp2 double-null cells may lack paraxial mesoderm properties. However, the analysis of adjacent sections suggests that *lacZ*-expressing Mesp1/Mesp2 double-null cells themselves express *Uncx4.1*, a somite-specific marker (Fig. 7C,D), and they had also been found to have normal expression of *Paraxis* (Fig. 6A,B).

It is believed that the rostro-caudal pattern within somites and dermomyotomes is generated in the PSM and maintained in somites and dermomyotomes. We observed a normal rostro-caudal pattern in the dermomyotome (Fig. 7), although wild-type cells and Mesp1/Mesp2 double-null cells are mixed in the PSM (Fig. 5), of Mesp1/Mesp2 double-null chimeric embryos. As Mesp products are required for suppression of *Dll1* in the anterior PSM, a normal Dll1 stripe pattern cannot be formed if Mesp1/Mesp2 double-null cells are randomly distributed in

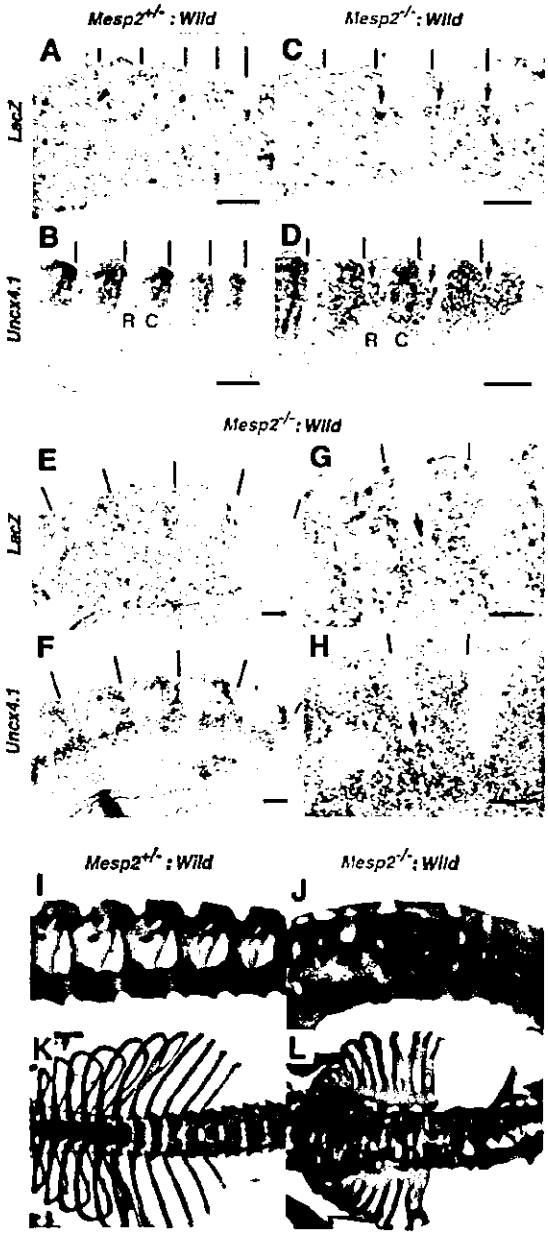

Fig. 4. Mesp2 function is cell autonomously required for rostral properties. (A-D) Expression of *lacZ* and *Uncx4.1* transcripts at the site of initial somite formation in control (A,B) and Mesp2-null (C,D) chimeric embryos. In the control, *lacZ*-expressing cells are randomly distributed and *Uncx4.1* expression is normal. In the Mesp2-null chimera, *lacZ*-expressing Mesp2-null cells at the rostral part of the incomplete segments (arrows in C) ectopically express *Uncx4.1* (arrows in D). Lines indicate somite boundaries. (E,F) In the dermomyotome, Mesp2-null cells are mostly localized at the caudal end, and the *Uncx4.1* expression pattern is normal. (G,H) In the sclerotome, the distribution of Mesp2-null cells results in expansion of *Uncx4.1* expression (arrows). (I) The control chimeric fetus shows normal vertebrae. (J) The Mesp2-null chimeric fetus exhibits partial fusion of the neural arches. (K) The control chimeric fetus shows normal ribs. (L) The Mesp2-null chimeric fetus shows proximal rib fusion. Scale bars: 100 μm. C, caudal compartment; R, rostral compartment.

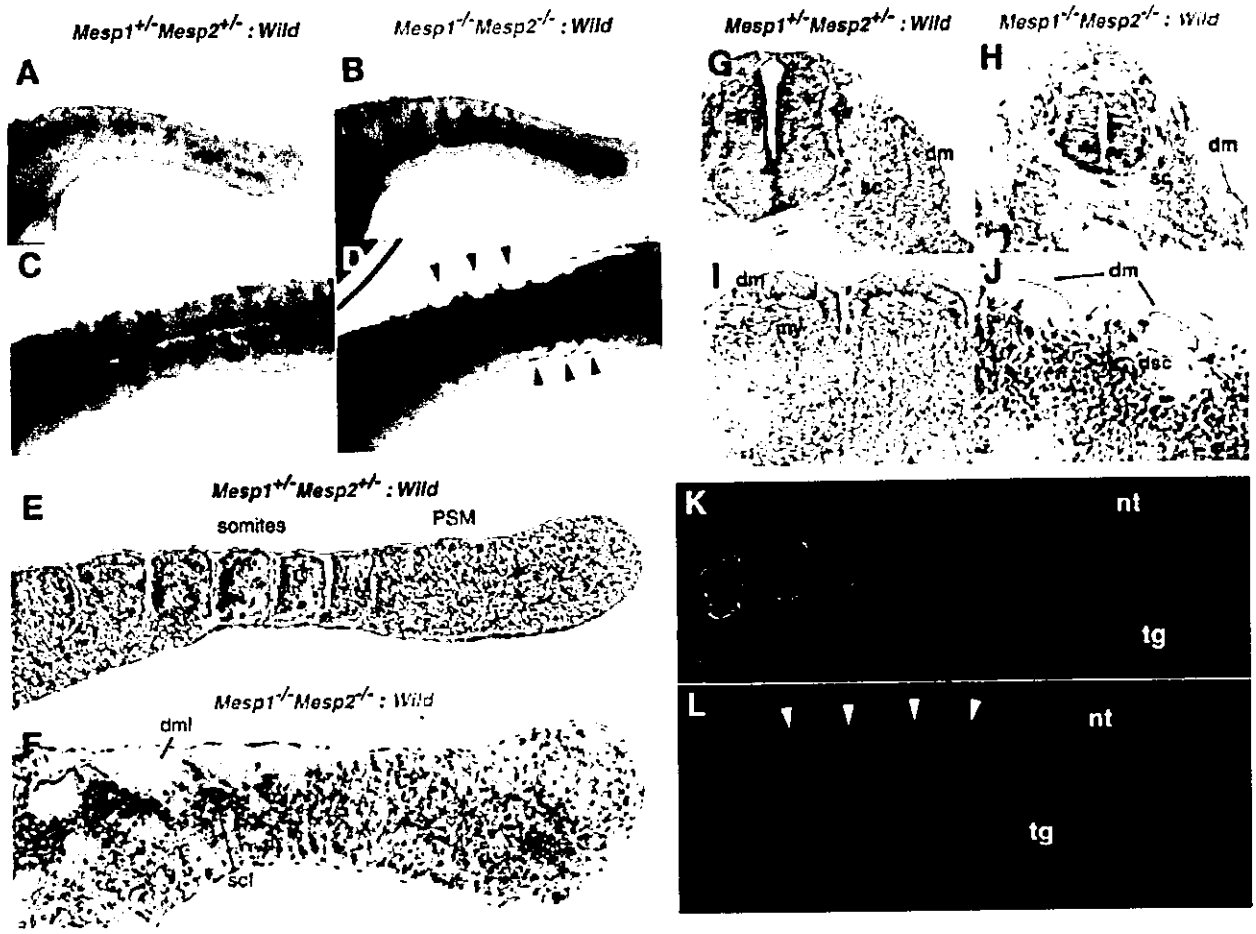

Fig. 5. Mesp1/Mesp2 double-null cells fail to contribute to epithelial somites or to the dermomyotome. (A-D) Tail regions from X-gal-stained whole-mount specimens of control (A,C) and double-null (B,D) chimeric embryos. (A,B) Lateral view. (C,D) Dorsal view. The blue double-heterozygous cells are randomly distributed in the control embryo, whereas the Mesp1/Mesp2 double-null cells are excluded from the lateral region of the somites (arrowheads in D). (E,F) Parasagittal sections of tails from chimeric embryos. (E) The labeled cells are randomly located in the control chimera. (F) The two types of cells are randomly mixed in the PSM, whereas the dermomyotome-like epithelium consisted exclusively of wild-type cells and the sclerotome-like compartment contained mostly Mesp1/Mesp2 double-null cells. Note that normal epithelial somites are not formed in this chimera. (G,H) Transverse sections show elimination of Mesp1/Mesp2 double-null cells from the dermomyotome. (I,J) The dermomyotome-like epithelium in the Mesp1/Mesp2 double-null chimeric embryo gives rise to dermomyotome, myotome (arrowhead in J) and the dorsal part of the sclerotome. Red arches indicate the inner surface of dermomyotome. (K,L) AlexaFluor 488-labeled phalloidin staining shows normal epithelialization of somites in the control chimera (K) and restriction of epithelialization in the dermomyotome-like compartment in the Mesp1/Mesp2 double-null chimera (L). dm, dermomyotome; dml, dermomyotome-like epithelium; dsc, dorsal part of the sclerotome; my, myotome; nt, neural tube; sc, sclerotome; scl, sclerotome-like compartment; tg, tail gut.

the anterior PSM. This is because 50% of cells cannot undergo suppression of Dll1 even in the future rostral half region. Therefore, our finding of a normal rostro-caudal pattern in the dermomyotome of double-null chimeras is surprising and raises the question of whether wild-type cells can be normally patterned in the presence of surrounding Mesp1/Mesp2 double-null cells. To determine how the rostro-caudal pattern in the dermomyotome is formed in the PSM, we examined the expression pattern of *Dll1* (Bettenhausen et al., 1995), the stripe expression profile of which is established in the anteriormost PSM via the function of Mesp2 (Takahashi et al., 2000). The *lacZ*-expressing Mesp1/Mesp2 double-null cells were subsequently found to be consistently localized in the sclerotome-like region, where *Dll1* expression was abnormally expanded (Fig. 6C,D). In the dermomyotome-like region, however, *Dll1* expression in the caudal half was normal. Intriguingly, strong *Dll1* expression in the anteriormost PSM was suppressed in a rostrally adjoining cell population, which is mainly occupied by wild-type cells (Fig. 6C,D, arrows). This implies that wild-type cells and Mesp1/Mesp2 double-null cells rapidly segregate at S-1 to S0, after which the rostro-caudal pattern of *Dll1* expression is formed in the partially segregated wild-type cell population but not in the randomly mixed cell population. In other words, the separation from Mesp1/Mesp2 double-null cells enabled normal rostro-caudal patterning of wild-type cells.

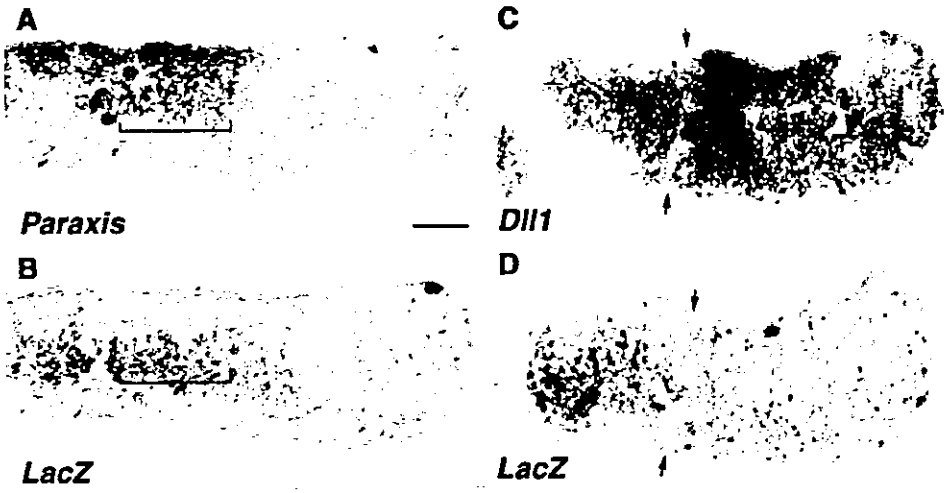

Fig. 6. (A,B) Mesp1/Mesp2 double-null cells express *Paraxis*. Adjacent parasagittal sections of the Mesp1/Mesp2 double-null chimeric embryo were stained for either *Paraxis* (A) or *lacZ* (B). Note that the expression domains of the two genes overlap in the medial sclerotomal region (brackets). (C,D) The rostro-caudal pattern in the dermomyotome is formed in a partially segregating wild-type cell population. Adjacent sections of the Mesp1/Mesp2 double-null chimeric embryos were stained for *Dll1* (C) or *lacZ* (D) mRNA. Red outlines demarcate the dorsal dermomyotome-like compartments. Note that suppression of *Dll1* expression occurs in a region mostly occupied by wild-type cells (arrows). Scale bar: 100 μm.

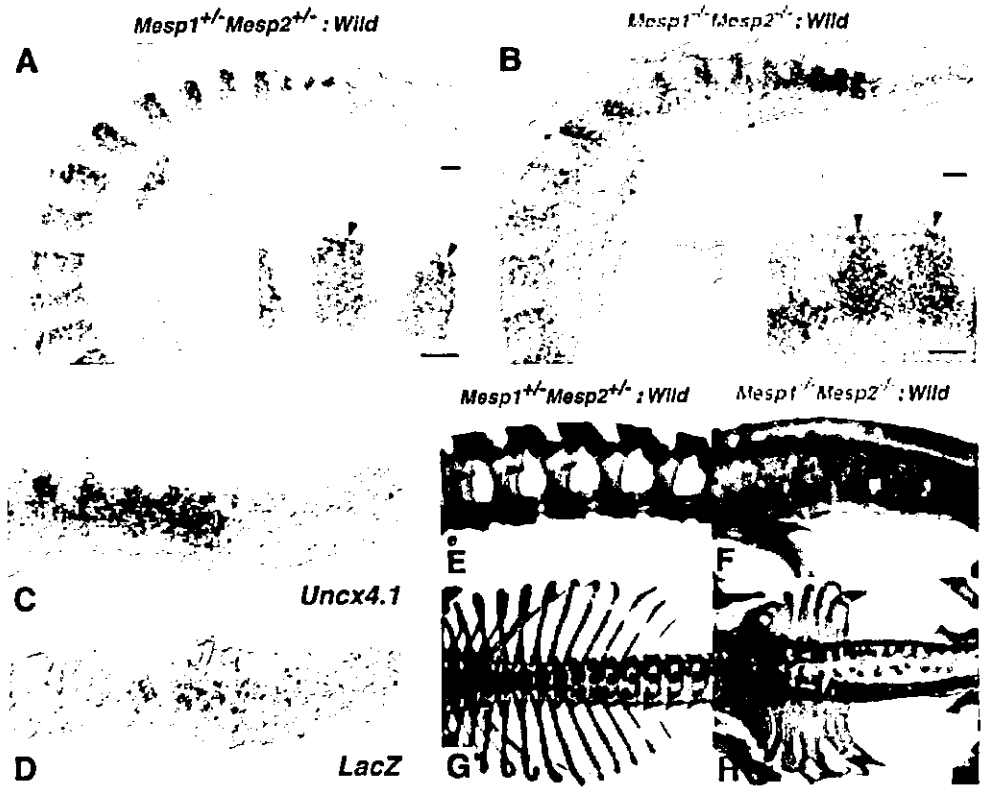

Fig. 7. Rostro-caudal patterning of the sclerotome is disrupted in Mesp1/Mesp2 double-null chimeric embryos. (A) The control chimeric embryos exhibit normal stripe patterns of *Uncx4.1* expression throughout the somite region. (B) The Mesp1/Mesp2 double-null chimeric embryos exhibit continuous *Uncx4.1* expression in the ventral sclerotomal region. Note that caudal localization of *Uncx4.1* expression is normal in the dermomyotome and dorsal sclerotome. The insets show a higher magnification of lumbar somites. (C,D) Adjacent sections showing that *lacZ*-expressing Mesp1/Mesp2 double-null cells express *Uncx4.1*. (E-H) The Mesp1/Mesp2 double-null chimeric fetus exhibits caudalization of the vertebrae and of the proximal ribs. (E) The control chimeric fetus shows normal metameric arrangement of the neural arches. (F) The Mesp1/Mesp2 double-null chimeric fetus shows severe fusion of the pedicles and the laminae of neural arches. (G) The control chimeric fetus has normal arrangement of ribs. (H) The double-null chimeric fetus shows severe fusion of the proximal elements of the ribs. Scale bars: 100 μm.

Mesp2-null fetuses display caudalized vertebrae with extensive fusion of the pedicles of neural arches and proximal elements of the ribs (Saga et al., 1997). The Mesp1/Mesp2 double-null chimeric fetuses also exhibited fusion of the pedicles of neural arches and the proximal ribs (Fig. 7E-H). Furthermore, the vertebrae of severe chimeric fetuses were indistinguishable from those of Mesp2-null fetuses. These observations indicate that Mesp1/Mesp2 double-null cells can differentiate into caudal sclerotome and possibly contribute to chondrogenesis.

Discussion

Mesp1 and Mesp2 not only exhibit similar expression patterns but also share common bHLH domains as transcription factors. Previous studies using gene replacement experiments (Saga, 1998) (Y.S. and S.K., unpublished) indicate that these genes can compensate for each other. However, the early lethality of double knockout mice hampered any further detailed analysis of somitogenesis. An obvious strategy to further elucidate the functions of Mesp1 and Mesp2 was, therefore, the generation of a conditional knockout allele for *Mesp2* in *Mesp1* disrupted cells in which the Cre gene is specifically activated in the paraxial mesoderm, which is now underway. Chimera analysis is also a powerful method as an alternative strategy. Comparisons of chimeras, composed of either Mesp2-null or Mesp1/Mesp2 double-null cells, made it possible to determine the contribution of Mesp1 to somitogenesis. Our results indicate that Mesp1 has redundant functions in the epithelialization of somitic mesoderm and additionally, by chimeric analysis, we were able to demonstrate the cell autonomy of Mesp1 and Mesp2 function during some critical steps of somitogenesis.

The relative contributions of Mesp1 and Mesp2 to somitogenesis

In Mesp1-null mice, epithelial somites with normal rostro-caudal polarity are generated, whereas Mesp2-null mice exhibit defects in both the generation of epithelial somites and the establishment of rostro-caudal polarity. Thus, it seems likely that Mesp2 function is both necessary and sufficient for somitogenesis. However, dermomyotome formation was observed, without normal segmentation, even in Mesp2-null mice. In view of the apparent redundant functions of Mesp1 and Mesp2 in somitogenesis, as demonstrated by our previous gene replacement study, it was possible that the Mesp1/Mesp2 double-null embryo would exhibit a much more severe phenotype in relation to somitogenesis. In our chimera analyses, both Mesp2-null and Mesp1/Mesp2 double-null cells exhibited complete caudalization of somitic mesoderm, indicating that Mesp1 function is not sufficient to rescue Mesp2 deficiency and restore rostro-caudal polarity. Likewise, both Mesp2-null and Mesp1/Mesp2 double-null cells were incapable of forming an initial segment boundary, showing that the contribution of Mesp1 is also minor during this process. By contrast, whereas Mesp1/Mesp2 double-null cells lacked any ability to epithelialize, Mesp2-null cells were occasionally integrated into epithelial somites and dermomyotome, indicating that the contribution of Mesp1 to epithelialization is significant and that Mesp1 can function in the absence of Mesp2 (Fig. 8). We therefore postulate that the epithelialization of dermomyotome, observed in Mesp2-null embryos, is dependent on Mesp1.

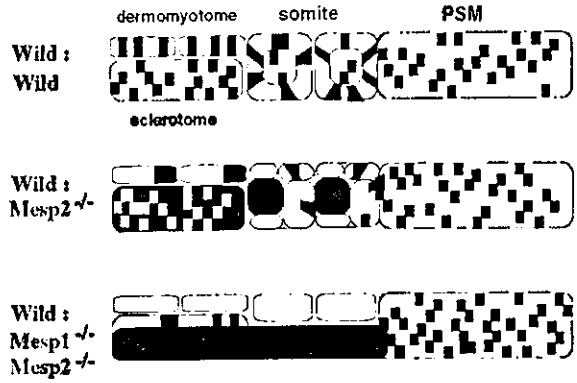

Fig. 8. A schematic summarization of the Mesp1/Mesp2 chimera experiments. Mesp1/Mesp2 double-null cells can contribute to neither epithelial somite nor dermomyotome formation, whereas Mesp2-null cells can partially contribute to both somites and dermomyotome. Red outlines indicate epithelialized tissues (epithelial somites, dermomyotomes and abnormal small clusters).

Mesp factors are cell autonomously required for epithelialization of somitic mesoderm but may also be non-cell autonomously required for morphological boundary formation

Conventional interpretations of the results of chimera analysis are generally based upon the regulative development of the vertebrate embryo and argue cell autonomy of specific gene functions in embryogenesis (Ciruna et al., 1997; Brown et al., 1999; Kitajima et al., 2000; Koizumi et al., 2001). Mesp1/Mesp2 double-null cells failed to form epithelial somites, even in the presence of surrounding wild-type cells. In addition, they were incapable of contributing to dermomyotome, where cell sorting occurs. This strongly suggests that Mesp factors are cell autonomously required for the epithelialization of somitic mesoderm. However, we also found striking non-cell autonomous effects of Mesp mutant cells on wild-type cell behaviors. That is, both types of Mesp mutant cell not only failed to undergo normal somitogenesis, but also inhibited the normal morphogenesis of wild-type cells. This implies that there are non-cell autonomous roles for Mesp factors in the establishment of the future somite boundary, as we will discuss further.

Initial epithelial somite formation is achieved by the mesenchymal-epithelial transition of cells located in the anterior PSM. A future somite boundary is established at a specific position in the PSM, followed by gap formation between the mesenchymal cell populations. Subsequently, cells located anterior to the boundary are epithelialized. This process is known to be mediated by an inductive signal from cells posterior to the boundary (Sato et al., 2002). Therefore, defects in epithelial somite formation can be explained in two principal ways: a lack of cellular ability to epithelialize (cell autonomous) and a lack of an inducing signal, which is produced in the anterior PSM by a mechanism mediated by Notch signaling (thus non-cell autonomous). In the case of chimeras of Mesp1/Mesp2 double-null cells, no local

boundary formed by locally distributed wild-type cells was observed, i.e. even a gap between wild-type cells was never observed in the mixture of Mesp1/Mesp2 double-null cells and wild-type cells. It is likely, therefore, that the wild-type cell population can form a boundary only after separation from Mesp1/Mesp2 double-null cells (Fig. 8). By contrast, some local boundaries between epithelial wild-type cell clusters were occasionally observed in chimeras with Mesp2-null cells. Considering that there is functional redundancy between these transcription factors, it is possible that either Mesp1 or Mesp2 is necessary for the formation of a signaling center or source of the putative inductive signal. Hence, we cannot exclude the possibility that the lack of Mesp function may affect non-cell autonomous generation of the inductive signal in the anterior PSM.

Formation of epithelial somites requires paraxis, which is a transcription factor (Burgess et al., 1996; Nakaya et al., 2004). We observed that Mesp1/Mesp2 double-null cells at the medial sclerotomal region expressed *Paraxis*, indicating that Mesp factors are not absolutely required for *Paraxis* expression. Defects in epithelial somite formation in paraxis-null embryos, with normal *Mesp2* expression (Johnson et al., 2001), and in Mesp2-null embryos, with normal *Paraxis* expression, imply that epithelial somite formation independently requires both gene functions.

Mesp2 is cell autonomously required for the acquisition of rostral properties

The distribution of Mesp2-null cells in the Mesp2-null chimeric embryos may appear somewhat paradoxical, as they are localized at the rostral side in the incomplete somites but at the caudal side in the dermomyotome. Initial localization at the rostral and central region, however, is likely to be due to the relative lack of epithelialization functions. In mammalian and avian embryos, mesenchymal-to-epithelial conversion of the PSM commences from the rostral side of the future somite boundary, i.e. the caudal margin of the presumptive somite (Duband et al., 1987). Epithelialization then proceeds anteriorly in the dorsal and ventral faces and in such a process, Mesp2-null cells, which are less able to participate in epithelialization, may therefore be pushed to the central and rostral sides. Thus, the majority of the Mesp2-null cells localize to the central, prospective sclerotomal region and a small number of them are integrated in the future dermomyotomal region. The incomplete somites then undergo reorganization into dermomyotome and sclerotome, and small numbers of Mesp2-null cells in the dermomyotome may be sorted out to the caudal end. Therefore, the apparently complex distribution pattern of Mesp2-null cells is likely to reflect a combination of defects in epithelialization and rostro-caudal patterning. In the incomplete segments of Mesp2-null chimeric embryos, the Mesp2-null cells fail to acquire rostral properties even when localized at the rostral side. Moreover, in the dermomyotome, where rostro-caudal patterning is rescued, Mesp2-null cells are mostly localized in the caudal region. These observations suggested that the requirement of Mesp2 for the acquisition of rostral properties is cell autonomous. Similarly, it has been reported that presenilin 1 (Psen1) is required for acquisition of caudal half properties (Takahashi et al., 2000; Koizumi et al., 2001) and that Psen1-null cells cannot contribute to the caudal half of somites in chimeric embryos, showing cell autonomous roles for Psen1 (Koizumi et al., 2001).

Mesp mutant cells affect the rostro-caudal patterning of somites due to the lack of cellular interaction with wild-type cells

In a previous study, we have shown that the rostro-caudal patterning of somites is generated by complex cellular interactions involved in positive and negative feedback pathways of Dll1-Notch and Dll3-Notch signaling, and regulation by Mesp2 in the PSM (Takahashi et al., 2003). In chimeras with either Mesp2-null or Mesp1/Mesp2 double-null cells, the mutant cells were distributed evenly and did not show any sorting bias in a rostro-caudal direction in the PSM. Since both Mesp2-null and Mesp1/Mesp2 double-null cells have the ability to form caudal cells, it is likely that if wild-type cells could occupy the rostral part of future somite regions and have the ability to sort in the PSM, a normal rostro-caudal patterning would be generated. We did not observe this, however, and conclude that the presence of mutant cells lacking Mesp factors must have disrupted normal cellular interactions via Notch signaling. Thus these non-cell-autonomous effects of our mutant cells are strongly supportive of our previous contention that rostro-caudal pattering is generated by cellular interactions via Notch signaling.

We thank Mariko Ikumi, Seiko Shinzawa, Eriko Ikeno and Shinobu Watanabe for general technical assistance. This work was supported by Grants-in-Aid for Science Research on Priority Areas (B) and the Organized Research Combination System of the Ministry of Education, Culture, Sports, Science and Technology, Japan.

References

Bettenhausen, B., Hrabe de Angelis, M., Simon, D., Guénet, J.-L. and Gossler, A. (1995). Transient and restricted expression during mouse embryogenesis of Dll1, a murine gene closely related to *Drosophila* Delta. *Development* **121**, 2407-2418.

Borycki, A. G. and Emerson, C. P., Jr (2000). Multiple tissue interactions and signal transduction pathways control somite myogenesis. *Curr. Top. Dev. Biol.* **48**, 165-224.

Brown, D., Wagner, D., Li, X., Richardson, D. A. and Olson, E. N. (1999). Dual role of the basic helix-loop-helix transcription factor scleraxis in mesoderm formation and chondrogenesis during mouse embryogenesis. *Development* **126**, 4317-4329.

Burgess, R., Cserjesi, P., Ligon, K. L. and Olson, E. N. (1995). Paraxis: a basic helix-loop-helix protein expressed in paraxial mesoderm and developing somites. *Dev. Biol.* **168**, 296-306.

Burgess, R., Rawls, A., Brown, D., Bradley, A. and Olson, E. N. (1996). Requirement of the *paraxis* gene for somite formation and musculoskeletal patterning. *Nature* **384**, 570-573.

Ciruna, B. G., Schwartz, L., Harpal, K., Yamaguchi, T. P. and Rossant, J. (1997). Chimeric analysis of *fibroblast growth factor receptor-1 (Fgfr1)* function: a role for FGFR1 in morphogenetic movement through the primitive streak. *Development* **124**, 2829-2841.

Duband, J. L., Dufour, S., Hatta, K., Takeichi, M., Edelman, G. M. and Thiery, J. P. (1987). Adhesion molecules during somitogenesis in the avian embryo. *J. Cell Biol.* **104**, 1361-1374.

Fan, C. M. and Tessier Lavigne, M. (1994). Patterning of mammalian somites by surface ectoderm and notochord: Evidence for sclerotome induction by a hedgehog homolog. *Cell* **79**, 1175-1186.

Gossler, A. and Hrabe de Angelis, M. (1997). Somitogenesis. *Curr. Top. Dev. Biol.* **38**, 225-287.

Johnson, J., Rhee, J., Parsons, S. M., Brown, D., Olson, E. N. and Rawls, A. (2001). The anterior/posterior polarity of somites is disrupted in Paraxis-deficient mice. *Dev. Biol.* **229**, 176-187.

Kitajima, S., Takagi, A., Inoue, T. and Saga, Y. (2000). MesP1 and MesP2

are essential for the development of cardiac mesoderm. *Development* **127**, 3215-3226.
Koizumi, K., Nakajima, M., Yuasa, S., Saga, Y., Sakai, T., Kuriyama, T., Shirasawa, T. and Koseki, H. (2001). The role of presenilin 1 during somite segmentation. *Development* **128**, 1391-1402.
Mansouri, A., Yokota, Y., Wehr, R., Copeland, N. G., Jenkins, N. A. and Gruss, P. (1997). Paired-related murine homeobox gene expressed in the developing sclerotome, kidney, and nervous system. *Dev. Dyn.* **210**, 53-65.
Nakaya, Y., Kuroda, S., Katagiri, Y. T., Kaibuchi, K. and Takahashi, Y. (2004). Mesenchymal-epithelial transition during somitic segmentation is regulated by differential roles of Cdc42 and Rac1. *Dev. Cell* **7**, 425-438.
Neidhardt, L. M., Kispert, A. and Herrmann, B. G. (1997). A mouse gene of the paired-related homeobox class expressed in the caudal somite compartment and in the developing vertebral column, kidney and nervous system. *Dev. Genes Evol.* **207**, 330-339.
Nieto, M. A., Gilardi-Hebenstreit, P., Charnay, P. and Wilkinson, D. G. (1992). A receptor protein tyrosine kinase implicated in the segmental patterning of the hindbrain and mesoderm. *Development* **116**, 1137-1150.
Nomura-Kitabayashi, A., Takahashi, Y., Kitajima, S., Inoue, T., Takeda, H. and Saga, Y. (2002). Hypomorphic *Mesp* allele distinguishes establishment of rostro-caudal polarity and segment border formation in somitogenesis. *Development* **129**, 2473-2481.
Pourquié, O. (2001). Vertebrate somitogenesis. *Annu. Rev. Cell. Dev. Biol.* **17**, 311-350.
Saga, Y. (1998). Genetic rescue of segmentation defect in MesP2-deficient mice by MesP1 gene replacement. *Mech. Dev.* **75**, 53-66.
Saga, Y. and Takeda, H. (2001). The making of the somite: molecular events in vertebrate segmentation. *Nat. Rev. Genet.* **2**, 835-845.
Saga, Y., Hata, N., Kobayashi, S., Magnuson, T., Seldin, M. and Taketo, M. M. (1996). MesP1: A novel basic helix-loop-helix protein expressed in the nascent mesodermal cells during mouse gastrulation. *Development* **122**, 2769-2778.
Saga, Y., Hata, N., Koseki, H. and Taketo, M. M. (1997). *Mesp2*: a novel mouse gene expressed in the presegmented mesoderm and essential for segmentation initiation. *Genes Dev.* **11**, 1827-1839.
Saga, Y., Miyagawa-Tomita, S., Takagi, A., Kitajima S., Miyazaki, J. and Inoue, T (1999). MesP1 is expressed in the heart precursor cells and required for the formation of a single heart tube. *Development* **126**, 3437-3447.
Sato, Y., Yasuda, K. and Takahashi, Y. (2002). Morphological boundary forms by a novel inductive event mediated by Lunatic fringe and Notch during somitic segmentation. *Development* **129**, 3633-3644.
Takahashi, Y., Koizumi, K., Takagi, A., Kitajima, S., Inoue, T., Koseki, H. and Saga, Y. (2000). Mesp2 initiates somite segmentation through the Notch signalling pathway. *Nat. Genet.* **25**, 390-396.
Takahashi, Y., Inoue, T., Gossler, A. and Saga, Y. (2003). Feedback loops comprising Dll1, Dll3 and Mesp2, and differential involvement of Psen1 are essential for rostrocaudal patterning of somites. *Development* **130**, 4259-4268.
Zambrowicz, B. P., Imamoto, A., Fiering, S., Herzenberg, L. A., Kerr, W. G. and Soriano, P. (1997). Disruption of overlapping transcripts in the ROSA beta geo 26 gene trap strain leads to widespread expression of beta-galactosidase in mouse embryos and hematopoietic cells. *Proc. Natl. Acad. Sci. USA* **94**, 3789-3794.

ELSEVIER

Mechanisms of Development 121 (2004) 1443–1453

www.elsevier.com/locate/modo

Mouse Nkd1, a Wnt antagonist, exhibits oscillatory gene expression in the PSM under the control of Notch signaling

Aki Ishikawa[a], Satoshi Kitajima[b], Yu Takahashi[b], Hiroki Kokubo[a], Jun Kanno[b], Tohru Inoue[b], Yumiko Saga[a,*]

[a]*Division of Mammalian Development, National Institute of Genetics, Yata 1111, Mishima 411-8540, Japan*
[b]*Cellular and Molecular Toxicology Division, National Institute of Health Sciences, 1-18-1 Kamiyoga, Setagayaku, Tokyo 158-8501, Japan*

Received 19 May 2004; received in revised form 29 July 2004; accepted 9 August 2004
Available online 16 September 2004

Abstract

During vertebrate embryogenesis, the formation of reiterated structures along the body axis is dependent upon the generation of the somite by segmentation of the presomitic mesoderm (PSM). Notch signaling plays a crucial role in both the generation and regulation of the molecular clock that provides the spatial information for PSM cells to form somites. In a screen for novel genes involved in somitogenesis, we identified a gene encoding a Wnt antagonist, Nkd1, which is transcribed in an oscillatory manner, and may represent a new member of the molecular clock constituents. The transcription of *nkd1* is extremely downregulated in the PSM of *vestigial tail* (*vt/vt*), a hypomorphic mutant of Wnt3a, whereas *nkd1* oscillations have a similar phase to *lunatic fringe* (*L-fng*) transcription and they are arrested in Hes7 (a negative regulator of Notch signaling) deficient embryos. These results suggest that the transcription of *nkd1* requires Wnt3a, and that its oscillation patterns depend upon the function of Hes7. Wnt signaling has been postulated to be upstream of Notch signaling but we demonstrate in this study that a Wnt-signal-related gene may also be regulated by Notch signaling. Collectively, our data suggest that the reciprocal interaction of Notch and Wnt signals, and of their respective negative feedback loops, function to organize the segmentation clock required for somitogenesis.

Keywords: Subtraction; Somitogenesis; Wnt signaling; Mesp2; Segmentation clock

1. Introduction

Somites are transient structures that are only observed during embryogenesis, and their reiterated nature in vertebrates is an important foundation for the generation of metameric structures such as vertebrae, ribs, spinal nerves and skeletal muscle. The somites are formed sequentially in an anterior to posterior direction, concomitant with the posterior extension of the tailbud. Once the paraxial mesoderm is generated from the tailbud, the cells are known to then be under the control of the segmentation clock (or molecular clock) and acquire periodic properties (Pourquié, 2001). Among the several genes that have been implicated in somitogenesis, those involved in the Notch signaling pathway are now known to play major roles. The experimental and genetic evidence that is now accumulating also indicates that Notch signaling is a component of the molecular clock that governs temporal control, and that it is also required for the establishment of the rostro-caudal polarity of somites within the presomitic mesoderm (PSM) prior to segment border formation (Takahashi et al., 2000). The molecular mechanisms underlying these events have recently begun to be more fully understood. There could, however, be additional genes and/or signaling pathways involved in somitogenesis. In fact, Wnt signaling is implicated in both the generation and maturation of tailbud cells (Takada et al., 1994), whereas FGF signaling has been shown to be important for the maintenance of immature PSM cells prior to segmentation (Dubrulle et al., 2001; Sawada, 2001).

Previously, we cloned the gene *Mesp2*, which encodes a bHLH-type transcription factor (Saga et al., 1997) and is

* Corresponding author. Tel: +81-559-81-6829; fax: +81-559-81-6828.
E-mail address: ysaga@lab.nig.ac.jp (Y. Saga).

0925-4773/$ - see front matter © 2004 Elsevier Ireland Ltd. All rights reserved.
doi:10.1016/j.mod.2004.08.003

transiently expressed in the rostral PSM (in either S-1 or S-2: we refer a forming somite as S0) before segment border formation occurs. Additionally, *Mesp2*-null mice show defective somitogenesis due to a lack of a rostral somitic compartment. Recent genetic analyses have also now revealed that *Mesp2* functions in a Notch-signaling feedback network (Takahashi et al., 2003). Mesp2 stimulates *Notch1* expression and suppresses *Dll1* expression, whereas both Notch 1 and Dll1 appear to be required for either the activation or maintenance of *Mesp2* expression. However, no direct targets of Mesp2 have yet been identified.

In order to identify putative downstream target genes of Mesp2 and to further elucidate the molecular mechanisms underlying the formation and maturation of PSM cells, which are required for somite segmentation, we generated two subtractive cDNA libraries and screened them by in situ hybridization (ISH). We subsequently obtained more than 30 clones that are expressed in either the somite, the PSM and/or the tailbud. Among these genes, we identified several known components of the Wnt signaling pathway, and we focused in particular on the mouse *nkd1* gene which is expressed in an oscillatory manner in the PSM. *nkd* is a homolog of the *Drosophila* segment polarity gene *naked cuticle* (*nkd*), which encodes an antagonist of Wg activity (Zeng et al., 2000). It has been shown that mouse Nkd1 can bind Dishevelled and antagonize canonical Wnt signaling (Yan et al., 2001a; Wharton et al., 2001). Furthermore, it has also recently been reported that *Axin2*, which encodes an inhibitor of Wnt signaling, exhibits a cyclic expression pattern during somitogenesis and may play a key role upstream of the segmentation clock generated by Notch signaling (Aulehla et al., 2003). Our comparative analyses of such cyclic genes suggest that *nkd1* is a component of these pathways that exhibits an oscillatory expression pattern, which may act as a link between the Notch and Wnt signaling cascades and contribute to the establishment of the segmentation clock.

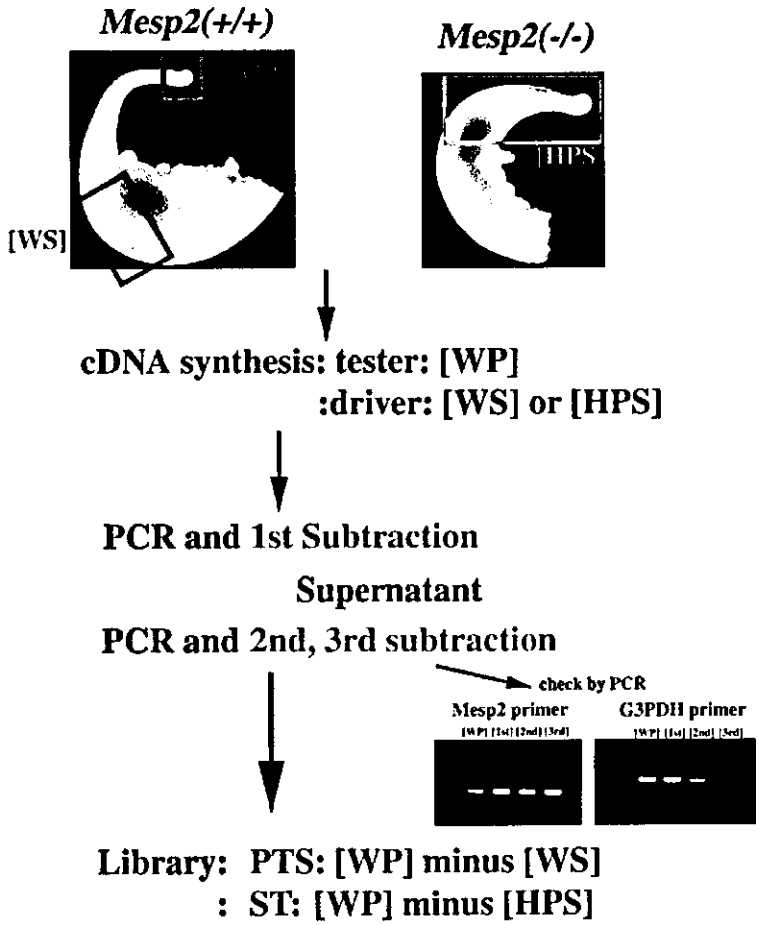

Fig. 1. Schematic representation of subtractive cDNA library protocols. Subtraction was carried out with cDNAs derived from the dissected portions of either wild-type (WP and WS) or Mesp2-null (HPS) 11.5 dpc embryos. Two different types of oligonucleotide linker-primers were utilized to prepare either tester or driver cDNAs. After three rounds of subtraction, the efficiency of the method was validated for the *Mesp2* (specific RNA to the PSM) and *G3PDH* (ubiquitous RNA) genes by PCR. After the cloning steps, we designated the generated subtractive libraries as PTS ([WP] minus [WS]) and ST ([WP] minus [HPS]).